Field-dependent nonlinear luminescence response of (In,Ga)N/GaN quantum wells

U. Jahn,* S. Dhar, and M. Ramsteiner
Paul-Drude-Institut für Festkörperelektronik, Hausvogteiplatz 5-7, D-10117 Berlin, Germany

K. Fujiwara
Kyushu Institute of Technology, Tobata, Kitakyushu 804-8550, Japan
(Received 13 November 2003; published 19 March 2004)

We have investigated the electric-field- and excitation-density-induced variation of the optical transition energy and cathodoluminescence (CL) as well as photoluminescence intensity of a single (In,Ga)N/GaN quantum well deposited in the depletion region of a *p-n* junction. The electric-field dependence of the transition energy is significantly influenced by field screening in the depletion region due to the excited carriers and by filling of band tail states of localized excitons. The electric-field dependence of the CL intensity is characterized by an abrupt and strong quenching mainly due to drift of excited carriers in the depletion region. A gradual screening of the *p-n* junction field with increasing excitation density causes a strongly nonlinear CL response. We describe this nonlinear behavior theoretically by a rate equation model.

DOI: 10.1103/PhysRevB.69.115323 PACS number(s): 78.67.De, 73.63.Hs, 78.55.Cr, 78.20.Bh

I. INTRODUCTION

The optical response of quantum wells (QW's) depends strongly on the electric field applied perpendicular to the layers via the quantum-confined Stark effect (QCSE), which causes both a red shift of the optical transition energy (E_t) and a reduction of the quantum efficiency (η).[1–3] Optical intensity modulators based on the QCSE make use of the electric-field-induced shift of E_t and hence of the excitonic absorption resonance. The intensity modulation is usually a result of the corresponding variation of the absorption coefficient.[4,5] Optically controlled light modulators combine the QCSE with electric-field screening by excited carriers.[6,7] A number of authors have reported a nonlinear optical response caused by excitation-density-dependent electric-field screening in GaAs/(Al,Ga)As (Refs. 6 and 8) and (In,Ga)As/GaAs (Refs. 7 and 9–11) QW systems.

Little is known about excitation-density-dependent screening effects and a corresponding nonlinear optical response of GaN-related QW's in an external electric field. (In,Ga)N/GaN QW's could be very interesting in this respect because of a large internal electric field mainly due to piezoelectric polarization.[12] However, a screening of the piezoelectric field of such QW's by carrier excitation is rather difficult, since it is expected to occur only for very high intensities.[13,14] Recently, Jho *et al.*[15] have investigated the electric-field dependence of the recombination dynamics in a light-emitting diode (LED) consisting of (In,Ga)N/GaN QW's. They found that for high electric fields, tunneling of carriers through the tilted barriers of the QW's becomes dominant. Thus, a field-induced modulation of the luminescence intensity can also be reached by other mechanisms than the QCSE such as tunneling, thermally activated sweep-out, and carrier drift.[15–17] As the tunneling and drift of carriers depend strongly on the electric field of the *p-n* junction, one should expect a significant impact of electric-field screening by excess carriers on the luminescence response in such structures. It is, therefore, of considerable interest from the viewpoint of both fundamental physics and practical application to investigate the influence of various quenching mechanisms on the optical response of (In,Ga)N/GaN QW's embedded in a *p-n* junction. Furthermore, the (In,Ga)N/GaN system is of special interest, since localization of QW excitons due to lateral potential fluctuations plays an important role.[18] Consequently, density-dependent screening effects are expected to be superimposed by the density-dependent occupation of localized and free-excitonic states.

Since the *p* region of an (In,Ga)N/GaN LED is usually situated on the top of the structure (surface side), the electric field of the *p-n* junction and the piezoelectric field of the QW's act in opposite directions. This configuration allows for an easy distinction between the impact of the QCSE on the one side and tunneling as well as drift on the other side on the quantum efficiency of the QW.

In this paper, we describe the dependence of the luminescence spectra of an (In,Ga)N/GaN single QW situated within a *p-n* junction on the electric field as well as on the excitation density. It is shown that for cathodoluminescence (CL) experiments, i.e., excitation of carriers above the energy of the QW barriers, drift of the carriers by the electric field of the *p-n* junction acts as a dominant quenching mechanism of the QW luminescence. Thus, for reverse bias and low forward bias voltages, the luminescence intensity is very weak. With increasing forward bias, the recovery of the CL intensity occurs very steeply within a voltage range smaller than 0.5 V. Moreover, the onset voltage, at which the recovery of the luminescence is observed, depends significantly on the excitation density. As a result, the optical response of the QW is strongly nonlinear. It turns out that for bias voltages within the onset range, the quantum efficiency increases with increasing excitation density because of the shift of the onset voltage towards lower values of the forward bias. However, for bias voltages outside of this range, an increasing generation rate leads to a reduction of η due to an increasing portion of free excitons compared with localized ones. We also describe this nonlinear behavior in detail by a rate equation model.

II. EXPERIMENT

For the present experiments, we used a commercially available light-emitting diode developed by Nakamura *et al.*[19] It consists of the following layer sequence fabricated by metal-organic chemical-vapor deposition on a sapphire substrate: a 30 nm thick GaN buffer, 4 μm *n*-type GaN, a 3 nm thick (In,Ga)N QW layer, 100 nm *p*-type (Al,Ga)N, and 500 nm *p*-type GaN. The nominal InN and AlN mole fractions were claimed to be 0.45 and 0.2, respectively. However, the InN mole fraction is probably overestimated. According to the value of E_t for the QW between 2.3 and 2.4 eV, the InN mole fraction is expected to be 0.25–0.3.[20] CL and electron-beam-induced current (EBIC) measurements were performed in a scanning electron microscope at 5 K. The beam energy amounted to 15 keV.

Investigations of the excitation-density dependence were carried out by varying either the electron-beam current or the excitation volume switching the beam from the focused to well-defined defocused states.[13] As a measure for the excitation density, we use the generation rate *G*, which is the number of electron-hole pairs excited by the electron beam per second per unit area *A*: $G=G_0/A$. An approach to estimate G_0 has been described in Ref. 13. For the focused electron beam, the area of excitation has been determined by calculating the lateral energy dissipation of the 15 kV electron beam in GaN using Monte Carlo simulations and by taking a diffusion length of the electron-hole pairs of 100 nm (Refs. 21 and 22) into account. The lateral width of electron scattering has been defined as the lateral distance with respect to the incident electron beam, at which the dissipated energy is decreased by a factor of 3. For the focused electron beam, we obtain a diameter of the excitation area of 0.5 μm and generation rates ranging from 3.6×10^{18} to 7.2×10^{20} cm^{-2} s^{-1}, when the beam current is varied between 1 and 200 pA. The variation of the beam current is limited by the signal-to-noise ratio on the low-current side and by electron-beam-induced modifications of the optical and electrical properties of GaN on the high-current side.[23]

Photoluminescence (PL) investigations were performed at 10 K using the 325 nm line of a HeCd laser for high-energy excitation and the 413 nm line of a Kr^+ ion laser for low-energy excitation.

III. RESULTS AND DISCUSSION

A. Field dependence of CL and PL spectra

In Fig. 1(a), we show the optical transition energy of the (In,Ga)N/GaN QW as a function of the bias voltage (U_{bias}). The symbols and the solid line depict the experimental data obtained from CL measurements and the theoretically expected ones, respectively. When U_{bias} is varied from 3 to -10 V, the experimental values of E_t increase by about 200 meV indicating the compensation of the piezoelectric field of the QW by the electric field of the *p*-*n* junction. The latter is composed of the built-in field and the electric field related to the applied bias voltage. Hereafter, the total electric field across the depletion region is called *p*-*n* junction field. There is a large deviation between the experimental data and the calculations, in particular, within the bias range between 0 and -10 V. We will return to this discrepancy later. For an (In,Ga)N/GaN QW without an external electric field, a compensation of the internal piezoelectric field leads to an increase of the quantum efficiency. Thus, the CL intensity (I_{CL}) is expected to increase by field compensation. In our case, the opposite is observed as shown in Fig. 1(b). With decreasing forward bias, the CL intensity (triangles) increases only between 3 and 2 V, but decreases abruptly for a further reduction of U_{bias}.

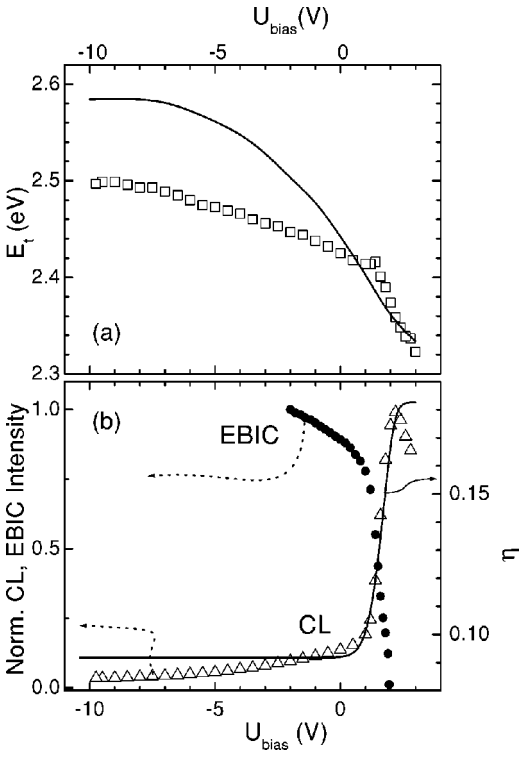

FIG. 1. (a) Optical transition energy (squares)—extracted from CL spectra—as a function of the bias voltage for the (In,Ga)N/GaN LED containing a single quantum well (SQW) at 5 K. (b) Normalized CL intensity (triangles) and EBIC signal (dots) as a function of the bias voltage at 5 K. The solid lines in (a) and (b) represent the results of calculations.

Already back in 1985, Horikoshi *et al.*[16] have shown that the PL quenching in reverse-biased GaAs/(Al,Ga)As QW's is due to carrier tunneling and carrier drift induced by the *p*-*n* junction field. Jho *et al.*[15] considered carrier sweep-out of the QW by tunneling and thermionic emission in order to explain the PL quenching in strained (In,Ga)N/GaN QW's with increasing reverse bias. Our observation of an increase of the EBIC signal [marked by dots in Fig. 1(b)] and a simultaneous decrease of the CL intensity suggests that the CL quenching mechanism is governed in this case by the carrier drift. The scenario is schematically sketched in Fig. 2(a). CL is induced by high-energy electrons resulting in an excitation of carriers far above the band-gap energy of the (Al,Ga)N barriers. Thus, for a reverse-biased *p*-*n* junction, electrons and holes can experience a drift, sweeping the holes and the electrons towards the *p* and *n* contact, respectively. Some of the electron-hole pairs are captured within the QW and con-

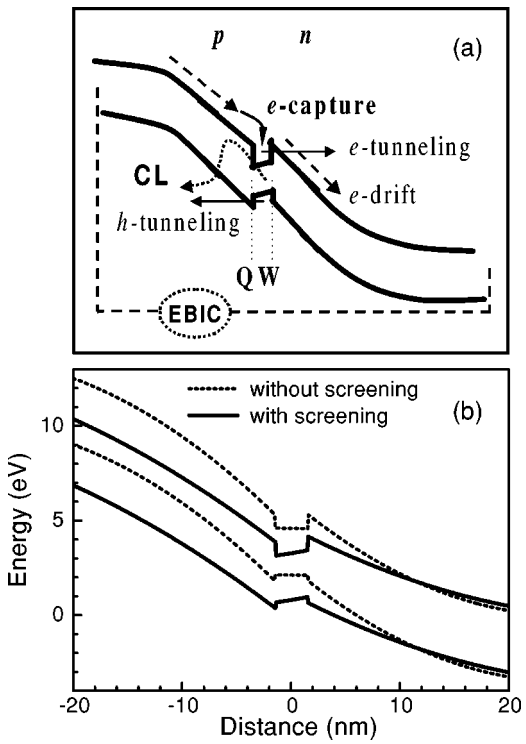

FIG. 2. (a) Sketch of the energy-band structure of a *p-n* junction containing a SQW. (b) Calculated band structure of a *p-n* junction containing a SQW. The band edges represented by dotted and solid lines have been calculated without and with taking screening of the *p-n* junction field into account, respectively. The bias voltage amounts to $U_{\mathrm{bias}}=-9$ V. For the screening condition, we assumed a carrier generation rate of $G=3.5\times10^{19}\ \mathrm{cm}^{-2}\,\mathrm{s}^{-1}$.

tribute to the CL signal, while some drift away, before being captured by the QW, and contribute to the EBIC signal. A fraction of captured carriers can tunnel through the barriers and contribute again to the EBIC. Both effects, drift and tunneling, can control the quantum efficiency in the well. At high reverse-bias voltages, the *p-n* junction field is high, leading to a large drift velocity of the carriers meaning a high escape rate on the one hand and on the other hand to a large tilt of the barrier potential meaning a high tunneling rate.

In order to clarify whether tunneling or drift dominates the CL quenching mechanism, we performed field-dependent PL measurements using different excitation energies. Figure 3 displays the corresponding results, where open and full squares represent the PL intensities for excitation well below and above the band-gap energy of GaN, respectively. Clearly, the electric-field dependencies of the PL intensities differ significantly from each other. Moreover, a distinct PL quenching showing a steep slope within the 2 to 1 V bias range is only observed for the above-band-gap excitation, which closely resembles the CL result. Consequently, we conclude that drift is the more dominant mechanism for CL quenching.

B. Model calculations

Under the excitation condition, we consider three types of carriers in the system: excess carriers in the barrier region

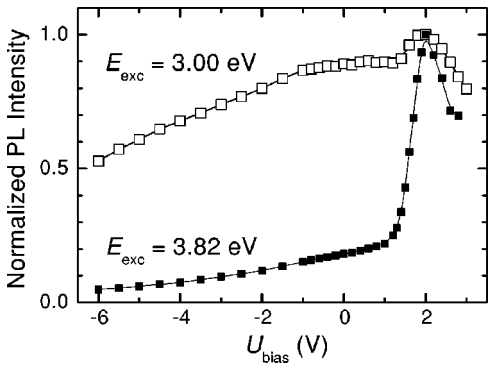

FIG. 3. Normalized PL intensity for excitation below (open) and above (solid squares) the band-gap energy of GaN for the (In,Ga)N/GaN LED containing a SQW as a function of the bias voltage at 10 K. E_{exc} denotes the energy of the laser light used for the PL excitation.

with the density n_b as well as free and bound excitons in the QW region with the densities n_w and n_t, respectively. The recombination dynamics of (In,Ga)N/GaN QW's is essentially determined by exciton localization, where the respective localization centers—hereafter called trap levels—are formed by growth-related fluctuations of the InN mole fraction in the well layer.[18] Thus, we have to distinguish between localized (or bound) and free excitons in the QW. The recombination dynamics of the excited carriers with a generation rate G is governed by the following three coupled rate equations describing the situation for the carriers in the barriers and for the free as well as bound excitons in the well:

$$G-b_{rw}n_b+b_{ew}n_w-g_bn_b=0, \tag{1}$$

$$G+b_{rw}n_b-b_{ew}n_w+b_{et}n_t-b_{rt}n_w(N_T-n_t)-(g_w+g_{nw})n_w=0, \tag{2}$$

$$b_{rt}n_w(N_T-n_t)-b_{et}n_t-g_tn_t=0. \tag{3}$$

For the sake of clarity, we have sketched the processes in Fig. 4. Moreover, all the symbols used in the rate equations

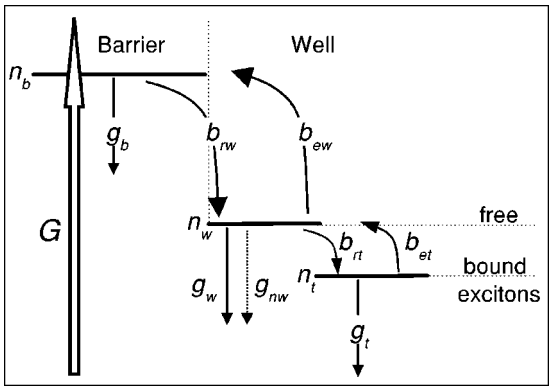

FIG. 4. Sketch of the processes included in the theoretical model, which describes the recombination dynamics in a QW for carrier excitation above the band-gap energy of the barriers.

are listed in Table I along with the corresponding explanations.

We consider that the densities of excess electrons and holes in the *n*- and *p*-type regions are the same (n_b) and are governed by Eq. (1). We neglect b_{ew} to decouple Eq. (1) from the others, which is a good approximation, particularly, at low temperatures, where thermally activated sweep-out of carriers is basically suppressed. Furthermore, tunneling out of the QW has been neglected, since we have seen that for CL (excitation far above the band-gap energy of the barrier) tunneling is affecting η much less than the drift of the carriers. Thus, our model focuses mainly on the relation between the drift within the field of the *p*-*n* junction and the capture probability of the excited carriers. The capture rate b_{rw} can be expressed as[24]

$$b_{rw} \propto \sigma_w v_d = b_o F \exp\left[-\frac{F}{F_c}\right], \tag{4}$$

where b_o and F_c are constants, and F is the electric field at the position of the QW. We assume that the cross section σ_w for capture of a carrier by the QW decreases exponentially with the increase of F and that the drift velocity v_d increases linearly with F: $\sigma_w \propto \exp[-F/F_c]$ and $v_d \propto F$. If we consider a QW just at the middle of a symmetric *p*-*n* junction with $N_A = N_D = N_i$, then $F = [qN_i'(V_{bi} - V)/\varepsilon]^{1/2}$, where N_A and N_D are the acceptor and donor concentrations, q is the electronic charge, ε the dielectric constant, V_{bi} the built-in voltage, V the voltage applied across the *p*-*n* junction, and $N_i' = N_i - n_b$. Equations (1) and (4) are solved to obtain n_b and b_{rw}.

Next, we utilize detailed balance between the thermal emission and capture rates of the excitons:[14]

$$\sigma = \frac{b_{rt}}{b_{et}} = \frac{1}{N_x} \exp \frac{E_b}{k_B T}, \tag{5}$$

where σ is the cross section for capture of an exciton by a trap level, E_b the localization energy, N_x the total density of the extended states, k_B the Boltzmann constant, and T the lattice temperature. To remove the (principally unknown) emission and capture coefficients, we next assume the validity of the above detailed balance criterion even under stationary conditions. While this assumption is strictly true only at high temperatures, it can be shown to be an excellent approximation even at low temperatures due to the exponential nature of σ. We thus obtain a simple analytical solution to Eqs. (2) and (3), which depends only on the recombination rates and σ.

We adopt the following conventions for the various recombination rates. g_b, g_t, and g_{nw} are assumed to be constant as a first approximation. The radiative recombination rate of free excitons may be expressed as $g_w = a/T$, where a is a constant. In principle a should be proportional to the integral of overlap between electron and hole stationary states. To obtain a, we should solve the Schrödinger and Poisson equations self-consistently along with these rate equations. We avoid this computational complexity by choosing a to be a constant. We will later discuss the range of validity of this approximation in our model. The rate equations (1)–(3) along with Eqs. (4) and (5) are solved to obtain n_b, n_t, and n_w. Finally, the quantum efficiencies η_w and η_t for free and bound excitons defined as $\eta_w = g_w n_w / G$, $\eta_t = g_t n_t / G$, and the total quantum efficiency of the QW $\eta = \eta_w + \eta_t$ were calculated.

TABLE I. Symbols used in the rate equations of the theoretical model.

Symbol	Explanation
b_{ew}	Emission rate of QW
b_{rw}	Capture rate of QW
b_{et}	Emission rate of traps
b_{rt}	Capture rate of traps
G	Generation rate
g_b	Recombination rate in barrier
g_w	Radiative recombination rate of free exciton in QW
g_t	Radiative recombination rate of bound exciton in QW
g_{nw}	Nonradiative recombination rate of free exciton in QW
n_b	Density of excited carriers in barrier
n_w	Density of free excitons in QW
n_t	Density of bound excitons in QW
N_T	Concentration of trap levels in QW

In Fig. 1(b), the calculated $\eta(U_{\text{bias}})$ is represented by the solid line. We did not try to fit the experimental data, since too many parameters of the investigated structure are unknown. We rather simulate η as a function of U_{bias} taking some meaningful values of the parameters listed in Table II into account, to qualitatively compare the experimental values with the calculated ones as it is shown in Fig. 1(b). Qualitative deviations are observed for high reverse and high forward bias voltages, where the experimental data indicate a decrease of the quantum efficiency with increasing U_{bias}, while the calculated η remains constant. For $U_{\text{bias}} > 2$ V, the qualitative deviation is due to the consequence of the approximation of treating a as a constant. At these voltages, free-excitonic recombination dominates the CL and hence $\eta_w \gg \eta_t$. The value of a and therefore η_w actually decrease with increasing bias voltage because of the QCSE. The impact of the QCSE is also apparent in Fig. 1(a) in the form of

TABLE II. Parameter values used for the calculation of the quantum efficiency η. $N_A = N_B = N_i$ denote the dopant concentrations, E_b the binding energy of the localized excitons, and N_T the concentration of the trap levels in the QW. b_o is a constant.

$N_A = N_B = N_i$ (cm^{-3})	g_w (s^{-1})	g_{nw} (s^{-1})	g_t (s^{-1})	g_b (s^{-1})	E_b (meV)	N_T (cm^{-2})	b_o (s^{-1})
1×10^{19}	1×10^{9}	1×10^{10}	9×10^{6}	1×10^{5}	25	1.4×10^{9}	7×10^{10}

TABLE III. Parameters used for the calculation of E_t. N_A and N_B denote the acceptor and donor concentration in the *p*- and *n*-type doped barrier, respectively. N_{AW}, N_{DW}, d_w, and x represent the acceptor concentration, the donor concentration, the thickness, and the InN mole fraction of the well layer, respectively. ΔE_C and ΔE_V denote the band offsets of the conduction and valance band between the well and barrier, respectively. Polarization fields of the QW are included according to Bernardini *et al.*[12]

$N_A=N_B=N_i$ (cm^{-3})	N_{AW} (cm^{-3})	N_{DW} (cm^{-3})	d_w (nm)	x	ΔE_C (eV)	ΔE_V (eV)
1×10^{19}	1×10^{15}	3×10^{17}	3	0.3	0.726	0.311

a red shift of E_t with increasing U_{bias} above 0 V. In Fig. 1(b), the deviation (for large reverse-bias voltages) is due to an increasing probability of carrier tunneling through the tilted barriers, which is also not taken into account in our model. The most distinct feature of the $I_{CL}(U_{\text{bias}})$ characteristics is, however, governed by the competition between carrier drift and capture and therefore well reflected by the calculated results.

We solve the Schrödinger and Poisson equations self-consistently to obtain the values of E_t. We assume a QW with a certain polarization field just at the middle of a symmetric *p*-*n* junction. The parameters used in this calculations are listed in Table III. The calculated values of E_t as a function of the bias voltage are represented by the solid line in Fig. 1(a). We have already mentioned that for reverse-bias voltages there is a large deviation from the experimentally obtained results. One reason for this deviation could be a partial screening of the *p*-*n* junction field by excited carriers, which has not been included in the calculation of $E_t(U_{\text{bias}})$. Indeed, screening of the *p*-*n* junction field has to be expected, since the excited electrons and holes are quickly separated by the field, which essentially suppresses the radiative recombination rate. Thus, as long as the excited electrons and holes are not captured by the QW (for $U_{\text{bias}}<1.5$ V) they contribute effectively to the screening of the electric field in the depletion region. However, once the excited carriers are captured by the QW (for $U_{\text{bias}}>1.5$ V), they cannot be separated by the *p*-*n* junction field, and screening is suppressed. The impact of screening of the *p*-*n* junction field on E_t of the QW becomes visible in Fig. 2(b) showing the calculated band structures with and without screening. We take the screening of the *p*-*n* junction field into account by replacing N_i by N_i'. Clearly, screening of the *p*-*n* junction field by excited carriers ($G=3.5\times10^{19}$ $cm^{-2}\,s^{-1}$) leads to a significant decrease of the compensation of the piezoelectric field in the QW. While without screening, the QW field is nearly compensated (the band is almost flat in the well region), the QW field is much less compensated under screening conditions. In the following, we consider the variation of $I_{CL}(U_{\text{bias}})$ and $E_t(U_{\text{bias}})$ with increasing excitation density, i.e., the influence of screening effects.

C. Excitation-density dependence

Figures 5(a) and 5(b) display the bias voltage dependence of E_t and I_{CL}, respectively, obtained for various values of the CL generation rate. For the sake of clarity, we have normalized the CL intensities to the respective maximum values. For the focused electron beam, the generation rate ranges from 3.6×10^{18} to 7.2×10^{20} $cm^{-2}\,s^{-1}$, when the beam current is varied between 1 and 200 pA, as indicated by the numbers in Fig. 5(a). The lowest generation rate of Fig. 5 ($\approx4\times10^{17}$ $cm^{-2}\,s^{-1}$) has been achieved by additionally defocusing the electron beam, i.e., by increasing the excitation area. For the defocused beam, the spot size has been determined as described in Ref. 13. The electric-field dependence of both the transition energy and the CL intensity varies significantly with excitation density.

E_t shows an overall blue shift with increasing generation rate. This blue shift can be attributed to the filling of the localized states by the increasing population in the QW. The screening of the piezoelectric field in the QW, which can also give rise to a blue shift, plays almost no role within the range of G values we have used in this study.[13,14] The carrier population can also be increased by bias-induced enhancement of

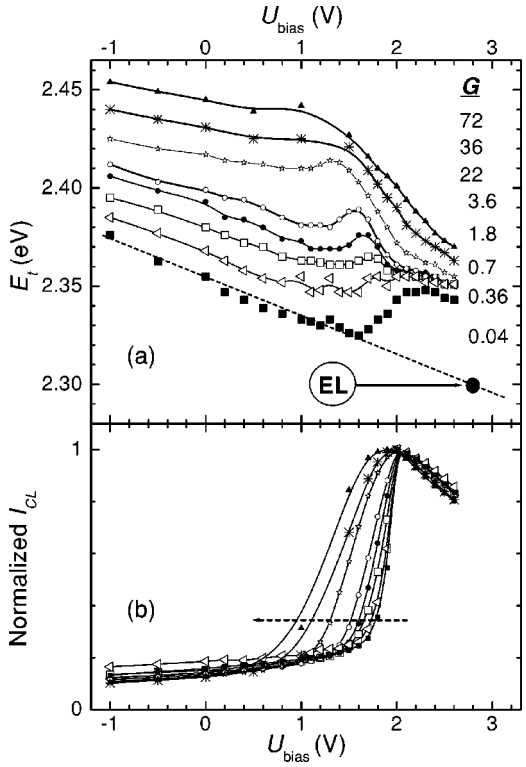

FIG. 5. (a) Optical transition energies and (b) normalized CL intensities as a function of the bias voltage for the (In,Ga)N/GaN LED containing a SQW. The various data sets differ in the CL generation rate, which is displayed in units of 10^{19} $cm^{-2}\,s^{-1}$ in (a). EL represents the onset energy of the electroluminescence of the LED.

the capture probability in the QW, as has been discussed earlier. This fact is clearly reflected in $E_t(U_{\text{bias}})$ for the lowest generation rate, where within a bias range of 1.5–2 V the red shift caused by the decreasing *p-n* junction field is inverted into a blue shift, which correlates well with the steep increase of I_{CL} indicating a steep increase of the capture probability for $U_{\text{bias}} > 1.5$ V. The bias dependence of E_t is basically governed by three competing processes: (i) the interaction of the piezoelectric field of the QW with the field of the *p-n* junction, (ii) the filling of band tail states, and (iii) a partial screening of the *p-n* junction field by the excited carriers as has been discussed above. The competition between the impact of the *p-n* junction field via the QCSE and the band tail filling via field-induced occupation of the QW can be directly observed within the bias range of 1–2 V, particularly, for low generation rates.

The onset of electroluminescence (EL) appears at $U_{\text{bias}} = 2.8$ V and exhibits a transition energy of 2.30 eV. This value agrees well with the extrapolated $E_t(U_{\text{bias}})$ of the lowest excitation density in Fig. 5(a) (dashed line). Indeed, an estimate of the corresponding EL generation rate can be obtained from the measured forward current of 0.3 μA. This value of about 10^{16} cm^{-2} s^{-1} is even lower than the smallest generation rate used for CL. The comparison of the CL and EL data nicely confirms the picture of localized carriers being mainly involved in the EL of such LED's.[25–27]

Another striking feature of increasing excitation density is a shift of the onset voltage of the $I_{CL}(U_{\text{bias}})$ curves towards lower forward bias voltages indicated by the dashed arrow in Fig. 5(b). The excitation-density-dependent shift of this onset voltage can also be easily understood in terms of a partial screening of the *p-n* junction field. Higher excitation density means more screening of the *p-n* junction field, which in turn means lower drift velocity and hence a higher cross section of the QW for carrier capture. The capture of carriers by the QW (the onset of the abrupt increase of the CL intensity) starts at lower forward bias for higher excitation densities. As a consequence, η of the QW significantly increases with increasing generation rate, when a bias voltage between 1 and 2 V is chosen. Within this bias range, the capture cross section of the QW increases steeply with decreasing drift field providing an efficient control of η by excitation-induced screening of the *p-n* junction field.

Figure 6(a) displays the ratio between the experimentally obtained CL intensity and the electron beam current (i_b), which is a measure for the quantum efficiency, as a function of U_{bias} for three values of G. In Fig. 6(b), we show the theoretically obtained $\eta(U_{\text{bias}})$ for various generation rates. As before, we only attempt to qualitatively compare the experimental data with the results of our model calculations by using meaningful values for the corresponding parameters (cf. Table II). Both experiment and theoretical model exhibit qualitatively the same dependence of η on U_{bias} and on G: The impact of G on the quantum efficiency is expected to be very different, when the bias voltage is varied. While for $1 < U_{\text{bias}} < 2$ V, η increases with increasing G, the quantum

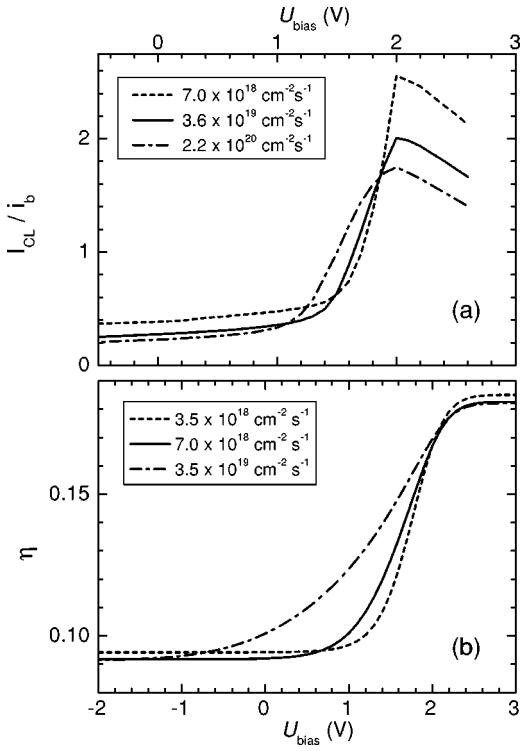

FIG. 6. (a) Measured CL intensity divided by the electron-beam current $[I_{CL}/i_b]$ and (b) calculated quantum efficiency for the (In,Ga)N/GaN QW LED as a function of the bias voltage for three distinct values of the CL generation rate. The latter are depicted in the graphs. Other parameters used for the calculations are listed in Table II.

efficiency is reduced for bias voltages outside of this range. In other words, the QW system exhibits a strongly nonlinear luminescence response.

We have also measured I_{CL} as a function of the generation rate for four values of the bias voltage. Figure 7 shows the corresponding ratio $[I_{CL}/i_b]$ as a function of G. For an increasing generation rate, $[I_{CL}/i_b]$ and therefore η are either reduced (at $U_{\text{bias}} = 2.1$ V) or increased (at $U_{\text{bias}} = 1.4$ and 1.65 V). At $U_{\text{bias}} = 0.8$ V, η firstly decreases, but increases again for very large generation rates indicating a strong shift of $I_{CL}(U_{\text{bias}})$ towards low forward bias voltages. The reduc-

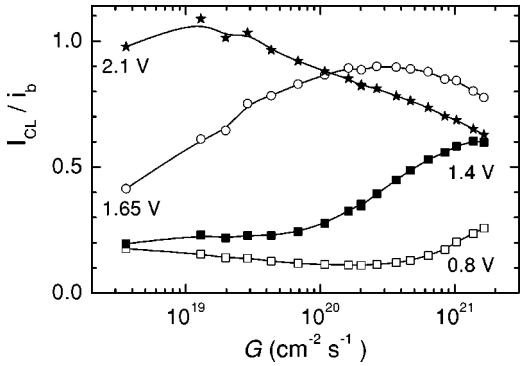

FIG. 7. CL intensity divided by the electron-beam current $[I_{CL}/i_b]$ for the (In,Ga)N/GaN QW LED as a function of the CL generation rate for four distinct values of the bias voltage.

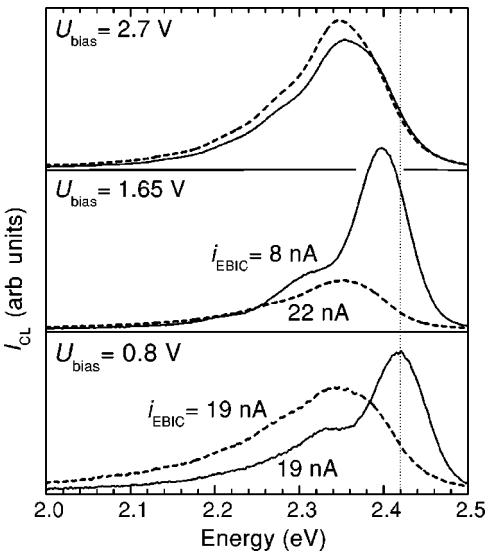

FIG. 8. CL spectra of the (In,Ga)N/GaN SQW deposited within a *p-n* junction for three distinct values of the bias voltage. Solid and dashed lines represent CL excitation by a focused and strongly defocused electron beam, respectively. The CL generation rate amounts to about 3×10^{20} cm^{-2} s^{-1} for the focused beam and is roughly two orders of magnitude less for the defocused beam. Additionally, the EBIC values measured at the bias voltages of 1.65 and 0.8 V are displayed.

tion of η observed for $U_{\text{bias}}>2$ V, where the flat-band condition of the depletion region is nearly reached, is due to an increasing portion of free excitons compared with localized ones, when the excitation density is increased.[14,13] The enhancement of η observed for $U_{\text{bias}}=1.4$ and 1.65 V is due to a partial screening of the *p-n* junction field and the resulting increase of σ_w as discussed above.

We have cross-checked the anomalous $\eta(G)$ behavior demonstrated in Fig. 7 by using an alternative method to vary the generation rate namely by increasing the excitation volume via a well-defined defocusing of the electron beam. When the current and energy of the beam are kept unchanged, the CL spectra provide a direct measure for the variation of η with varying excitation density in this manner. As an example, Fig. 8 shows CL spectra obtained at bias voltages of 2.7, 1.65, and 0.8 V. Solid and dashed lines represent CL excitation by a focused and strongly defocused electron beam, respectively. The generation rate of the focused beam amounts to 3×10^{20} cm^{-2} s^{-1}. The one of the defocused beam is about two orders of magnitude lower. For 2.7 V (*p-n* flat-band case is nearly achieved), an increase of the excitation density leads to a small decrease of η. The situation is significantly different, when a bias voltage of 1.65 V is chosen. Now, an increase of the excitation density leads to an enhancement of η by a factor of 2.7 and to a blue shift of the CL spectrum. At the same time, the EBIC signal decreases by a factor of 2.75. Therefore, the CL intensity clearly increases at the expense of the EBIC indicating the competition among carrier capture and carrier drift. For 0.8 V, the increase of the excitation density causes a blue shift of the CL spectrum as expected, where both the EBIC signal and the quantum efficiency remain almost unchanged. This set of CL spectra confirms nicely the trends observed in Fig. 7 and demonstrate again the strong density dependence of η within the bias range, in which luminescence quenching occurs. Moreover, the variation of the spectra shape with increasing excitation density, particularly for $U_{\text{bias}}=1.65$ and 0.8 V, can be interpreted in terms of filling as well as saturation of localized and occupation of free exciton states in the QW. For the low excitation density (defocused electron beam), the capture probability of the QW is small and most of the captured excitons can occupy localized states (trap levels) in the well. For the high excitation density (focused electron beam), the *p-n* junction field is partially screened leading to a significant enhancement of σ_w, which in turn yields a high exciton concentration and therefore a saturation of localized band tail states in the QW. As a result, the maximum of the CL spectrum shifts towards higher energies. In this sense, the high-energy part of the CL spectra obtained by excitation with the focused beam can be considered as a contribution of mainly free excitons, whereas the low-energy shoulder—clearly visible for $U_{\text{bias}}=1.65$ and 0.8 V—represents probably the contribution of localized exciton states. For increasing forward bias, the red shift of the free-exciton CL is due to the enhancement of the piezo-electric field in the QW.

The observed nonlinearities of the luminescence response of the LED-QW structure have at least to be taken into account, when intrinsic recombination properties are investigated by density-dependent measurements. One can also make use of such nonlinearities, e.g., for optical modulation purposes.

IV. CONCLUSIONS

In conclusion, the optical response of a single (In,Ga)N/GaN QW deposited in the depletion region of a *p-n* junction is strongly nonlinear, i.e., depends significantly on the excitation density and on the applied bias voltage. For a decreasing electrical field within the depletion region, the piezoelectric field of the QW gradually recovers resulting in a red shift of E_t. Once the field in the depletion region has been reduced down to a certain value, the probability of carrier capture within the QW increases steeply, and filling of band tail states of localized excitons results in a blue shift of E_t in competition with the red shift due to the QCSE.

PL excitation below and above the band-gap energy of the barriers revealed that for the high-energy excitation, the luminescence efficiency is essentially influenced by drift of the carriers caused by the *p-n* junction field. Thus, the electric-field dependence of the CL intensity is mainly governed by the drift of excited carriers resulting in an abrupt quenching of the intensity if the field of the depletion region exceeds a certain value. Consequently, for low forward and for reverse-bias voltages, the CL intensity is very weak. The forward bias voltage, at which a recovery of the quenched CL intensity is observed, shifts towards lower values, when the excitation density is increased. Corresponding model calculations show that a screening of the *p-n* junction field by the excited

carriers is responsible for this generation-rate-related shift of $I_{CL}(U_{\mathrm{bias}})$. Thus, for U_{bias} values situated within the onset range of the CL recovery, the quantum efficiency rises significantly with increasing excitation density. Outside this critical bias range, the opposite dependence of η on the excitation density is observed.

ACKNOWLEDGMENTS

We would like to thank H. Kostial and A. Kawaharazuka for the assistance in the sample processing and in the photoluminescence measurements as well as for valuable discussions.

*Electronic address: ujahn@pdi-berlin.de

[1] E.E. Mendez, G. Bastard, L.L. Chang, L. Esaki, H. Morkoç, and R. Fischer, Phys. Rev. B **26**, 7101 (1982).
[2] G. Bastard, E.E. Mendez, L.L. Chang, and L. Esaki, Phys. Rev. B **28**, 3241 (1983).
[3] D.A.B. Miller, D.S. Chemla, T.C. Damen, A.C. Gossard, W. Wiegmann, T.H. Wood, and C.A. Burrus, Phys. Rev. B **32**, 1043 (1985).
[4] D.A.B. Miller, Opt. Eng. **26**, 368 (1987).
[5] G.D. Boyd, D.A.B. Miller, D.S. Chemla, S.L. McCall, A.C. Gossard, and J.H. English, Appl. Phys. Lett. **50**, 1119 (1987).
[6] K. Obata, M. Yamanishi, Y. Yamaoka, Y. Kan, J. Hayashi, and I. Suemune, Appl. Phys. Lett. **57**, 419 (1990).
[7] I. Sela, D.E. Watkins, B.K. Laurich, D.L. Smith, S. Subbanna, and H. Kroemer, Appl. Phys. Lett. **58**, 684 (1991).
[8] Y. Abe, Y. Tokuda, K. Kanamoto, and N. Tsukada, Appl. Phys. Lett. **60**, 1664 (1992).
[9] S. Fafard, E. Fortin, and J.L. Merz, Phys. Rev. B **48**, 11 062 (1993).
[10] X.R. Huang, D.R. Harken, A.N. Cartwright, D.S. McCallum, A.L. Smirl, J.L. Sanchez-Rojas, A. Sacedon, F. Gonzalez-Sanz, E. Calleja, and E. Munõz, J. Appl. Phys. **76**, 7870 (1994).
[11] J.P.R. David, T.E. Sale, A.S. Pabla, P.J. Rodriguez-Girones, J. Woodhead, R. Grey, G.J. Rees, P.N. Robson, M.S. Skolnick, and R.A. Hogg, Appl. Phys. Lett. **68**, 820 (1996).
[12] F. Bernardini, V. Fiorentini, and D. Vanderbilt, Phys. Rev. B **56**, R10 024 (1997).
[13] U. Jahn, S. Dhar, O. Brandt, H.T. Grahn, and K.H. Ploog, J. Appl. Phys. **93**, 1048 (2003).
[14] S. Dhar, U. Jahn, O. Brandt, P. Waltereit, and K.H. Ploog, Appl. Phys. Lett. **81**, 673 (2002).
[15] Y.D. Jho, J.S. Yahng, E. Oh, and D.S. Kim, Phys. Rev. B **66**, 035334 (2002).
[16] Y. Horikoshi, A. Fischer, and K. Ploog, Phys. Rev. B **31**, 7859 (1985).
[17] I.A. Pope, P.M. Smowton, P. Blood, J.D. Thomson, M.J. Kappers, and C.J. Humphreys, Appl. Phys. Lett. **82**, 2755 (2003).
[18] B. Monemar, J.P. Bergman, J. Dalfors, G. Pozina, B.E. Sernelius, P.O. Holtz, H. Amano, and I. Akasaki, MRS Internet J. Nitride Semicond. Res. **4**, 16 (1999).
[19] S. Nakamura, M. Senoh, N. Iwasa, S. Nagahama, T. Yamada, and T. Mukai, Jpn. J. Appl. Phys., Part 2 **34**, L1332 (1995).
[20] S.F. Chichibu, T. Sota, K. Wada, S.P. DenBaars, and S. Nakamura, MRS Internet J. Nitride Semicond. Res. **4S1**, G2.7 (1999).
[21] Z.Z. Bandic, P.M. Bridger, E.C. Piquette, and T.C. McGill, Appl. Phys. Lett. **73**, 3276 (1998).
[22] J.C. Gonzalez, K.L. Bunker, and P.E. Russel, Appl. Phys. Lett. **79**, 1567 (2001).
[23] U. Jahn, S. Dhar, H. Kostial, I. M. Watson, and K. Fujiwara, Phys. Status Solidi C **0**, 2223 (2003).
[24] V. Ryzhii, M. Ryzhii, and H.C. Liu, J. Appl. Phys. **92**, 207 (2002).
[25] S. Chichibu, T. Azuhata, T. Sota, and S. Nakamura, Appl. Phys. Lett. **69**, 4188 (1996).
[26] P.G. Eliseev, P. Perlin, J. Lee, and M. Osinski, Appl. Phys. Lett. **71**, 569 (1997).
[27] T. Mukai, M. Yamada, and S. Nakamura, Jpn. J. Appl. Phys., Part 2 **37**, L1358 (1998).